Composites Science and Technology 72 (2012) 708–715

Contents lists available at SciVerse ScienceDirect

Composites Science and Technology

journal homepage: www.elsevier.com/locate/compscitech

Mechanisms and impact of fiber–matrix compatibilization techniques on the material characterization of PHBV/oak wood flour engineered biobased composites

Wil V. Srubar III [a,*], Srikanth Pilla [a], Zachary C. Wright [b], Cecily A. Ryan [a], Joseph P. Greene [c], Curtis W. Frank [b], Sarah L. Billington [a]

[a] Department of Civil and Environmental Engineering, Stanford University, Building 540, MC: 3037, Stanford, CA 94305-3037, USA
[b] Department of Chemical Engineering, Stanford University, Stauffer III, MC: 5025, Stanford, CA 94305-5025, USA
[c] Department of Mechanical Engineering, Mechatronic Engineering, and Manufacturing Technology, California State University, Chico, O'Connell 422, Chico, CA 95929-0798, USA

ARTICLE INFO

Article history:
Received 26 May 2011
Received in revised form 7 December 2011
Accepted 24 January 2012
Available online 2 February 2012

Keywords:
B. Mechanical properties
A. Particle-reinforced composites
A. Coupling agents
B. Fiber/matrix bond
C. Modeling

ABSTRACT

Fully biobased composite materials were fabricated using a natural, lignocellulosic filler, namely oak wood flour (OWF), as particle reinforcement in a biosynthesized microbial polyester matrix derived from poly(β-hydroxybutyrate)-*co*-poly(β-hydroxyvalerate) (PHBV) via an extrusion injection molding process. The mechanisms and effects of processing, filler volume percent (vol%), a silane coupling agent, and a maleic anhydride (MA) grafting technique on polymer and composite morphologies and tensile mechanical properties were investigated and substantiated through calorimetry testing, scanning electron microscopy, and micromechanical modeling of initial composite stiffness. The addition of 46 vol% silane-treated OWF improved the tensile modulus of neat PHBV by 165%. Similarly, the tensile modulus of MA-grafted PHBV increased 170% over that of neat PHBV with a 28 vol% addition of untreated OWF. Incorporation of OWF reduced the overall degree of crystallinity of the matrix phase and induced embrittlement in the composites, which led to reductions in ultimate tensile stress and strain for both treated and untreated specimens. Deviations from the Halpin–Tsai/Tsai–Pagano micromechanical model for composite stiffness in the silane and MA compatibilized specimens are attributed to the inability of the model both to incorporate improved dispersion and wettability due to fiber–matrix modifications and to account for changes in neat PHBV and MA-grafted PHBV polymer morphology induced by the OWF.

1. Introduction

Fully biobased polymeric materials are being engineered for target applications in the construction industry to address growing environmental concerns of a globally unsustainable dependence on non-renewable petroleum-based resources and to counter the proliferation of synthetic plastics in the environment. Among the most promising and well-characterized biobased polymers are polyhydroxyalkanoates (PHAs), aliphatic, semi-crystalline thermoplastic biopolyesters. PHA is biosynthesized in microbes that produce and store the polymer as energy-reserve inclusions in the cytoplasm when exposed to excess carbon sources typically under specific nutrient–deficient conditions [1]. PHA is of particular interest for it has been shown that copolymers can be synthesized from carbon-based sources such as glucose and methane [2] and that PHA-based materials anaerobically biodegrade in simulated landfill environments into methane gas [3], which can be sequestered and used either as a biofuel or as the closed-loop carbon source for further PHA production.

Poly(β-hydroxybutyrate) (PHB), the most commonly synthesized PHA, is highly crystalline and is comparable in material properties to isotactic polypropylene. Exhibiting excellent biocompatibility and biodegradability, PHB is currently used in niche biomedical and tissue engineering applications; however, PHB's applicability to other industries is limited due to high cost, a narrow thermal processing window, low impact strength, and brittleness [4]. PHB blends and copolymers with hydroxyvalerate (HV) such as poly(β-hydroxybutyrate)-*co*-poly(β-hydroxyvalerate) (PHBV), which is the focus of the work presented here, have been shown to improve thermal processability, decrease initial stiffness, and increase impact strength and ductility with increased HV comonomer content [5].

In addition to improving mechanical performance and reducing overall material cost, the use of natural fibers as functional fillers in wood–plastic composites in construction applications has gained favor due to attributes such as rapid renewability, low cost and density, high specific stiffness and strength, biodegradability, global abundance, and a potential for worldwide economic

* Corresponding author. Tel.: +1 650 723 4125; fax: +1 650 723 7514.
E-mail address: wsrubar@stanford.edu (W.V. Srubar III).

0266-3538/$ - see front matter © 2012 Elsevier Ltd. All rights reserved.
doi:10.1016/j.compscitech.2012.01.021

viability. Despite the proven ability of PHAs to better disperse fibers in two-phase lignocellulosic composite systems in comparison to petroleum-based plastics [6], natural fiber reinforcements exacerbate composite moisture absorption, which leads to fiber swelling, composite dimensional instability, matrix cracking, mass loss, and an increase in susceptibility to biodeterioration [6,7]. Furthermore, moisture uptake leads to a decrease in composite stiffness due to moisture-induced reductions in polymer crystallinity via plasticization, lowered glass transition temperatures, and hydrolysis-induced polymer chain scission and biodegradation [8].

Various physical and chemical fiber–matrix compatibilization techniques have been employed to improve both the mechanical performance and moisture resistance of natural fiber composites through an enhancement of the interfacial bond. Common compatibilization techniques include fiber modifications such as surface fibrillation, acetylation, dewaxing, cyanoethylation, and silanation, as well as matrix modifications such as maleic anhydride (MA) graft copolymerization [9]. Coupling agents containing silane or isocyanate reactive functional groups can react with fiber hydroxyls and/or the polymer matrix, thus improving interfacial adhesion. Matrix grafting has been used to modify the fiber–matrix surface energy leading to increased fiber wettability and, correspondingly, improved fiber dispersion. A comprehensive review of fiber–matrix interfacial characteristics and chemical compatibilization techniques for natural fiber-reinforced plastics can be found in Wu et al. [10] and George et al. [9].

Previous studies have investigated the effects of various modifications on the performance of natural fiber composites. Javadi et al. [11] and Shanks et al. [12] investigated the effect of silane on coir and flax fiber PHA-based composites, respectively. Thiodiphenol [13], butyric acid [14], pyridine [14], and acrylic acid [15] have also been used as chemical natural fiber treatments in PHA composites. The physical and mechanical impacts of MA grafting on PHB/wood flour [16] and kenaf fiber [17] composites have been studied, as well as the effects of MA-grafted PHBV on the crystallization behavior of PHBV/bamboo composites [18].

The research presented herein is part of a comprehensive characterization of a subset of fully biobased composites wherein the benefits of two fiber and matrix interfacial modifications for increased in-service mechanical performance (stiffness, strength) and long-term durability (low moisture absorption, thermal stability, UV resistance) are ultimately balanced with tradeoff effects on the rates of out-of-service anaerobic biodegradation.

For the primary characterization phase of this investigation, biobased composite specimens of PHBV with a reinforcing filler of natural, lignocellulosic oak wood flour (OWF) were fabricated using an extrusion–injection molding process. Mechanical and thermodynamic properties were characterized as a function of OWF loading by volume percent (vol%). The effects of a novel fiber-silane thermochemical vapor deposition treatment for wood flour and a MA matrix graft copolymerization technique were also investigated and correlated with the morphology of the altered fiber–matrix interface using scanning electron microscopy (SEM) and differential scanning calorimetry (DSC). Experimental results were compared with theoretical models for initial composite stiffness using the Halpin–Tsai/Tsai–Pagano micromechanical model to further investigate the induced phenomenological effects of the silane coupling agent and MA-grafting on the fiber–matrix interface.

2. Materials and methods

2.1. Materials

PHBV was obtained from Tianan Biological Materials Company, Zhejiang, China, under the trade name ENMAT™ Y1000P, in a pelletized form suitable for injection molding. Prior to processing, the PHBV was dried in a 50 °C oven for a minimum of 12 h to remove any moisture. After drying, it was found that PHBV pellets contained a maximum ambient moisture content less than 0.5% by weight. The density of PHBV has been reported to vary within 1.20–1.29 g/cm^3 dependent upon HV content and processing technique employed [19]; immersion experiments based on Archimedes' principle substantiated a PHBV density of 1.21 g/cm^3.

OWF was supplied by American Wood Fibers, Schofield, Wisconsin, USA under the trade name 2037-Oak. Fiber sieve analysis and volumetric measurements confirmed a 20 mesh OWF particle size <841 μm and an apparent (bulk) density of 0.44 g/cm^3. Optical microscopy of OWF confirmed a pre-processing average aspect ratio of 3.6. The OWF, which was found to have an ambient moisture content of 7.2%, was conditioned in an oven overnight at a temperature of 100 °C to remove the moisture prior to processing and stored until commencement of the compound extrusion process. For the silane treatment and MA reactive extrusion, trimethoxy(octadecyl)-silane, 2.5-Furandione (maleic anhydride, stored under vacuum), dicumyl peroxide, and phenolphthalein were obtained from Sigma–Aldrich.

2.2. Fiber–matrix compatibilization techniques

2.2.1. Silane thermochemical vapor deposition

A thermochemical vapor deposition technique was developed for the treatment of wood flour to ensure that silane was sufficiently chemisorbed onto the OWF particles. Prior to composite processing, 100 g batches of OWF were placed in glass, foil-lined desiccators. Above the OWF, 2 mL of silane were placed in a small aluminum tray. The desiccators were sealed and placed in a National Appliance 5831 vacuum-assisted oven operated at 120 °C and 95 kPa below atmospheric pressure for 24 h. At the end of the thermochemical treatment, 1 g samples of OWF were extracted from the bottom of the desiccator and tested with a drop of distilled water from a pipette to verify the hydrophobicity of the treated fibers. If any amount of the water droplet was absorbed by the fibers, the OWF-filled desiccator was placed back into the oven and tested for hydrophobicity periodically in 3 h increments. The solubility of silane in ethanol was verified; thus, random OWF samples were subsequently refluxed with ethanol and retested for hydrophobic behavior to ensure silane was covalently bound to the fiber surface.

2.2.2. MA-grafting via reactive extrusion

Using a Brabender Plasti-Corder single-screw extruder, MA was grafted onto the PHBV polymer chains via a reactive extrusion technique. A dry blend of PHBV pellets, MA, and dicumyl peroxide (10% and 0.75% of PHBV by weight, respectively) was fed through the main hopper. During extrusion, nitrogen gas was used to purge the hopper, which was sealed to prevent any side reactions from occurring between the blended materials and atmospheric oxygen. The reactive extrusion was performed at a melt temperature of 160 °C and an extruder screw speed of 20 rpm, which corresponded to a residence time of 150 s. Following reactive extrusion, the material was collected at the end of the die and uniformly pelletized by a Scheer Bay BT-25 pelletizer. The unreacted MA was removed by extracting the extruded material in acetone for 24 h using a soxhlet extractor. The extracted material was subsequently dried in an oven for 24 h before being subjected to acid–base titration using phenolphthalein as an indicator. The graft percentage was found using:

$$G = \frac{V_b N_b - V_a N_a - V_{net}}{2 w_x} \quad (1)$$

where G is the graft percentage (%), V_b is the base titrate volume (L), N_b is the base normality (0.02 mol/L), V_a is the acid titrate volume (L), N_a is the acid normality (0.02 mol/L), w_{mol} is the molecular weight of anhydride (98.06 g/mol), and w_x is the weight of titrated material (g). According to the literature, MA graft percentages attained for PHA-based polymers have been shown to range from 0.2 to 1.18% [16,18,20]. In this study, the graft percentage of MA-grafted PHBV (mPHBV) in the extracted material was determined to be 0.8%.

2.3. Composite processing

To investigate the effects of filler volume fraction and various fiber treatments on composite mechanical performance, three families of PHBV/OWF composites were processed. These composites included neat PHBV/untreated OWF (P), neat PHBV/silane-treated OWF (PS), and 2% mPHBV/untreated OWF (2M). Each family of composite was reinforced with varying amounts of OWF. Target fiber loadings ranged from 0 to 40% in 10% increments by weight percent of filler. Specimen nomenclature was derived from composite family classification (P, PS, 2M) and target fiber loading percent (10, 20, 30, 40).

2.3.1. Compound extrusion

Master batches of composite materials were fabricated using various quantities of the four material constituents: PHBV, untreated OWF, silane-treated OWF, and mPHBV. The target composite mixtures were formulated by compound extrusion using an American Leistritz ZSE-18HP twin-screw extruder set at a processing temperature of 165 °C and a main screw speed of 190 rpm. The screw diameter was set at 18 mm, and the length-to-diameter (l/d) ratio was 40:1. PHBV was fed into the main feed throat using a gravimetric feeder at a rate of 10%of the total flow rate of the extruder; the OWF was fed using a manual side screw at a rate of 38 rpm. The extruded composite was fed from the die into a cooling water bath and immediately pelletized into uniformly sized pellets, using a Scheer Bay BT-25 pelletizer.

2.3.2. Injection molding

Prior to injection molding, the compounded pellets were dried in an oven at 40 °C for 12 h to remove any residual moisture absorbed during pelletization. After oven-drying, American Society for Testing of Materials (ASTM) standard specimens for testing of tensile mechanical properties [21] were prepared using an Arburg 320A injection-molding machine. The screw diameter was set at 19 mm and the l/d ratio was 25:1. In order to reduce thermal degradation and to improve melt strength, the five heating zones of the machine barrel were fixed at 5 °C increments starting with 170 °C near the feed throat. The injection speed, pressure, and mold temperature were set to 95 mm/s, 121 MPa, and 50 °C, respectively. The average cycle time for the molding process was approximately 45 s.

2.4. Materials testing and characterization

2.4.1. Physical properties

The cross-sectional geometry (width and thickness) was measured on all composite tensile specimens. As previously discussed, the density of pure PHBV was measured by immersion of oven-dry samples in water according to ASTM D792 and calculated based on Archimedes' principle [22]. The densities of the PHBV/OWF composites were measured using the same standard. The density of the OWF functional filler was back-calculated using:

$$\frac{1}{\rho_c} = \left(\frac{w_f}{\rho_f}\right) + \left(\frac{1 - w_f}{\rho_p}\right) \quad (2)$$

where ρ_c is the composite density (g/cm^3), w_f is the actual weight percent of OWF, ρ_f is the OWF density (g/cm^3), and ρ_p is the measured polymer density (1.21 g/cm^3).

2.4.2. Weight percent

Due to use of a manual compound extrusion feeding method, a definitive target weight percent of OWF could not be guaranteed in the resultant injection-molded composite. Thus, ASTM D3171 [23] was used to determine the OWF weight fraction of the composite specimens. Solvent selection was based on the chemical composition of both matrix and filler, so as to dissolve the matrix and to leave the OWF intact. Chloroform was selected as the reagent in the modified dissolution method to adequately determine the OWF weight percent.

To guarantee the existence of no soluble constituents in the pure OWF, a 2 g sample of OWF was dissolved in chloroform. The dissolution test resulted in less than 0.59% loss of mass, thus substantiating the accuracy of the dissolution method employed.

2.4.3. Scanning electron microscopy (SEM)

Composite specimens were imaged using a FEI XL30 Sirion SEM to investigate filler morphology, fiber–matrix interfacial adhesion, and particle dispersion. Microscopy specimens were frozen using liquid nitrogen and immediately fractured both transversely and longitudinally in respect to the direction of the injection mold fill flow. The samples were attached to an SEM specimen mount with DAG-T-502 carbon paint and coated with Au60Pd40 alloy using a Gressington sputter coater operated at a current of 20 mA for 45 s. Detailed SEM micrographs were obtained using an acceleration voltage of 5 kV.

2.4.4. Differential scanning calorimetry (DSC)

A Perkin Elmer DSC 7 differential scanning calorimeter fitted with a dry ice-pure isopropanol cooler and a nitrogen purge gas chamber was used to determine the thermal properties of the polymer composites. The viscous cooling bath mixture was maintained at the dry ice sublimation temperature of −78 °C. Polymer and composite samples of 10–15 mg were equilibrated at 50 °C for 5 min before being heated from −50 °C to 185 °C at the rate of 3 °C/min and subsequently crystallized at a rate of 20 °C/min to room temperature.

Melting temperature, T_m, was found using analytical techniques based on the peak temperatures of the melting endotherm. Furthermore, the heat of melting, ΔH_m, was obtained via numerical integration of the melting peak, and crystallinity was determined by comparing the obtained ΔH_m with the theoretical heat of melting for 100% crystalline PHBV, 143 J/g [24]. The data were adjusted based on the wt% of polymer in the composite samples.

2.4.5. Tensile mechanical properties

The tensile specimens were tested according to ASTM D638-08 [21]. Testing was performed using an MTS 858 tabletop machine with a 13.5 kN capacity. Modulus of elasticity, ultimate strength, and maximum strain for the specimens were determined. Loading was displacement controlled using a crosshead speed of 5 mm/min. The longitudinal and transverse strains were measured using a 50 mm gage length extensometer and a strain gage, respectively.

3. Experimental results and discussion

3.1. Effects of processing

3.1.1. Thermal degradation in samples

Thermal degradation of the OWF was evident in the color disparities of the injection-molded samples. The composite

specimens varied in tint from light to dark brown depending upon the OWF content, whereas the silane-treated and MA compatibilized samples were even darker for the same OWF contents. Wood particles are thermally stable up to 200 °C [25]; however, at such elevated processing temperatures and pressures, the OWF particles may have been thermally degraded. Similar color change observations in natural fiber composites have been noted and attributed to the formation of (a) tar from the thermal degradation of hemicellulose and/or (b) black char powder due to pectin degradation; the crystalline structural integrity of cellulose, however, has been shown to remain unaffected below temperatures of 200 °C [26].

Four of 42 tested specimens contained a micropore approximately 0.6 mm in diameter, which accounted for less than 0.7% of the cross sectional area of the sample. Such spherical voids formed during processing most likely resulted from the existence of residual moisture in the OWF and/or polymer, which was evaporated during processing and entrapped in the polymer melt. Given the rare occurrence and minimal size of these micropores, the bulk density measurements and average mechanical properties were not adjusted to account for the reduction in cross sectional area.

3.1.2. Measured and observed composite/filler density

The density of pure PHBV was found via water immersion to be 1.21 g/cm^3 at room temperature. The overall density of preprocessed 20 mesh natural OWF particles is documented to range from 0.32 to 0.72 g/cm^3 [25]. The densities of the PHBV/OWF composites, however, resulted in an increase in composite density from 1.21 g/cm^3 to 1.22–1.30 g/cm^3 dependent upon fiber loading. The experimental determination of OWF density in the composite yielded an average value of 1.44 g/cm^3. Similar results in both injection-molded and extruded wood flour composites have been reported in the literature [13,16].

The phenomenological basis for the increase in composite density is due to the compressibility of wood flour particles. During processing, the OWF is exposed to elevated temperatures and pressures, which leads to (1) the collapse of the wood cell walls or (2) the forcing of matrix material through wood fiber lumens. These two mechanisms result in increased densities of the final composite, with the filler density effectively equal to the OWF cell wall density. Substantiating this phenomenon, the density of wood cell walls is documented to be 1.44–1.50 g/cm^3 contingent upon the wood specie [25].

SEM micrographs of liquid nitrogen-fractured surfaces of PHBV/OWF specimens are shown in Fig. 1. The images together confirm the collapse of individual OWF particles (Fig. 1a) and suggest phenomenological evidence of matrix infill of a partially collapsed OWF lumen (Fig. 1b).Comparatively, the average diameter of an uncollapsed oak wood lumen is approximately 8 μm [27].

3.1.3. Measured volume percent

As previously noted, the manual feed process employed during composite processing did not ensure target weight or volume concentrations. An accurate and thorough evaluation of the effects of fiber loadings on mechanical properties mandates the determination of actual weight percents of the fiber–matrix composite constituents. The results from the chloroform dissolution procedure are given in Table 1. Since it is more conventional to relate filler fractions in terms of volume instead of weight, the measured vol% is presented.

3.2. Mechanical characterization

3.2.1. Impact of fiber loading on untreated composites

The experimental results for the uniaxial tensile modulus of elasticity and ultimate strength characterization of neat PHBV and untreated PHBV/OWF composites are shown in Fig. 2a.The stiffness and strength properties for silane- and MA-treated specimens presented in Fig. 2b will be discussed in Section 3.2.2.

The tensile modulus of elasticity of the untreated composites, calculated as the initial slope of the stress–strain relationship, increased with an increase in OWF loading. For example, the addition of 18 and 36 vol% OWF increased neat PHBV stiffness by 114 and 127% from 3800 ± 102 MPa to 4320 ± 213 MPa and 4820 ± 180 MPa, respectively. The addition of OWF systematically decreased the ultimate composite tensile strength of neat PHBV from 34.8 ± 0.7 MPa to 21.4 ± 1.8 MPa with a fiber loading of 36 vol%. This corresponds to an average strength decrease of 3.4 MPa with every 5% OWF added by volume. Furthermore, the ultimate strain of neat PHBV shown in Fig. 3 was reduced with increased fiber loading. Maximum elongation decreased by one-half from 1.6% for neat PHBV to 0.8% with the addition of 36 vol% OWF.

As can be seen from the obtained DSC experimental results presented in Table 2, the overall crystallinity of the neat PHBV matrix decreased with increasing wood flour content for the untreated specimens. For example, the crystallinity of PHBV in the P40 composite was 10% less than neat PHBV. From the DSC thermograms shown in Fig. 4a, the reduced heat of melting, shift in melting temperature, and emergence of double melting peaks suggest a less-perfect arrangement of polymer crystal structures as wood flour is added to the PHBV matrix. Studies have shown that wood flour acts as a nucleating agent, promoting the rapid formation of transcrystalline structures along fiber surfaces during crystallization from the melt [11]. The reductions in overall polymer crystallinity are likely to have resulted from the introduction of discontinuities in the matrix crystal structure caused by the disordered growth of crystals at the fiber–matrix interface and their impingement on crystals forming in the bulk.

The reductions in strength and elongation in the untreated specimens are attributed to an embrittlement caused by improper fiber wetting that resulted in an incongruous fiber–matrix

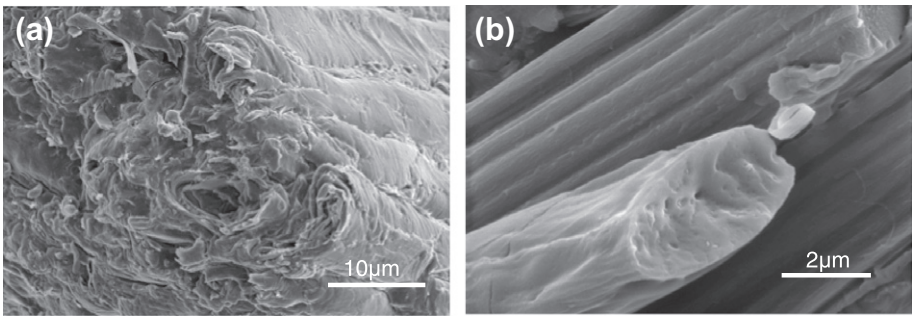

Fig. 1. SEM images of (a) collapsed wood fiber and (b) PHBV-filled lumen after fiber pullout.

Table 1
PHBV/OWF composite formulation: measured vol% after chloroform dissolution.

Constituent material	Sample nomenclature													
	P	P10	p20	P30	P40	PS10	PS10	PS20	PS30	PS40	2M10	2M20	2M30	2M40
Neat PHBV	100	91.6	82.4	73.8	63.8	92.3	81.5	71.6	53.6	98	89.3	79.7	69.9	55.6
MA-Grafted PHBV										2	2	2	2	2
Untreated OWF	–	8.4	17.6	26.2	36.2	-	–	–	–	–	8.7	18.3	28.1	42.4
Silane-Treated OWF	–	–	–	–	–	7.7	18.5	28.4	46.4	–	–	–	–	–

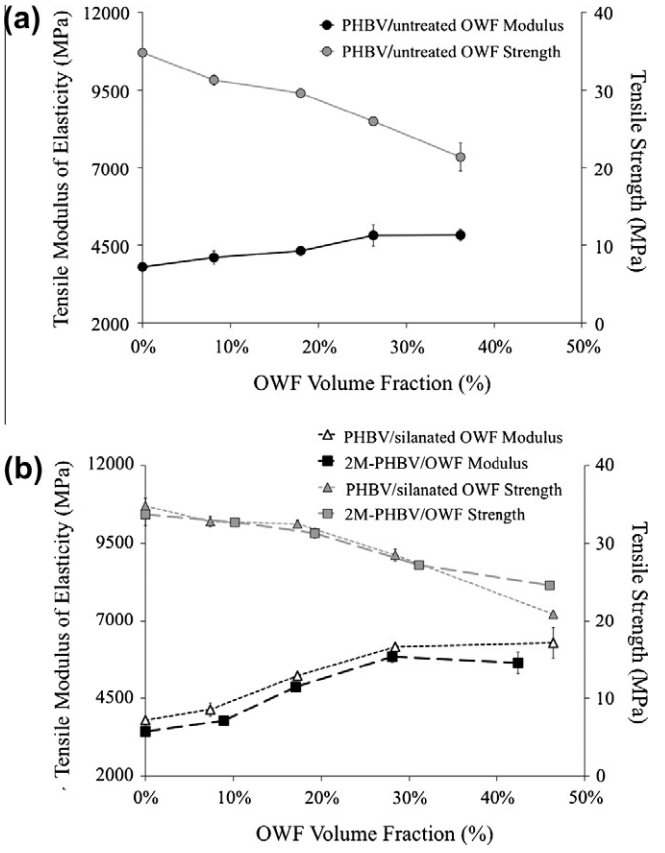

Fig. 2. Effect of (a) fiber loading and (b) fiber loading and chemical compatibilization technique on tensile modulus and tensile strength of PHBV/ OWF composites. Each data point represents the average tensile properties of three (3) specimens. The error bars represent ± one standard deviation.

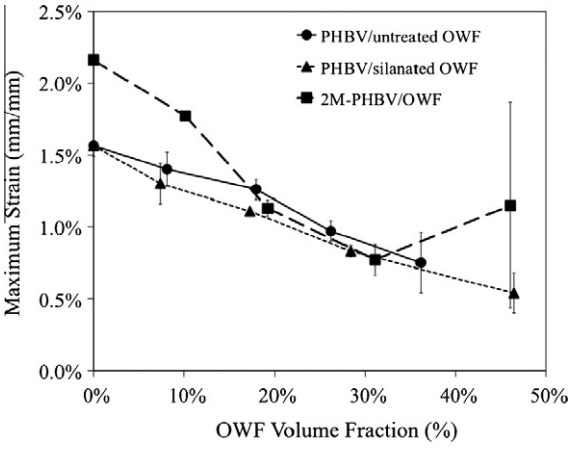

Fig. 3. Effect of fiber loading and chemical compatibilization technique on elongation to break of PHBV/OWF composites. Each data point represents the average tensile properties of three (3) specimens. The error bars represent ± one standard deviation.

Table 2
Obtained DSC results for melting temperature and crystallinity for the polymer–matrix in untreated, silane-treated, and MA-treated wood flour PHBV with varying wood flour vol%.

Sample	T_m (°C)	Polymer crystallinity (%)
PHBV	172.4	58.4
P10	171.9	58.3
P20	171.3	56.2
P30	172.5	54.3
P40	171.3	52.1
P10S	171.6	57.9
P20S	172.6	52.9
P30S	171.2	52.6
P40S	170.7	49.1
mPHBV	173.2	56.6
2M10	171.3	57.4
2M20	172.5	51.8
2M30	171.4	53.5
2M40	171.2	57.2

interface. The SEM micrograph of untreated wood flour and neat PHBV in Fig. 5a clearly shows the incompatibility between fiber and matrix. Such flaws and imperfections can induce fracture in highly crystalline polymers [10]. Compared to continuous fibers, wood fibers lack sufficient lengths to trigger toughening mechanisms that impede brittle fracture [28,29].

3.2.2. Impact of fiber–matrix compatibilization

From Figs. 2b and 3 it can be seen that the silane-treated and MA-grafted PHBV/OWF composites also exhibited increases in composite stiffness and decreases in ultimate strength and elongation-to-break with increases in OWF content. However, both treated specimens achieved higher increases in stiffness and lesser decreases in strength and ultimate strain than the untreated composites. The tensile modulus of neat PHBV was improved ~165% via addition of 46 vol% silane-treated OWF, whereas the tensile modulus of elasticity of the neat MA-grafted PHBV was improved ~170% by incorporating 28 vol% OWF. SEM micrographs of the fiber–matrix interface suggest that the marked gains in composite stiffness and preservation of strength can be attributed to an improvement in OWF particle wettability and dispersion achieved through compatibilization. As can be seen in Fig. 5b, better wetting was achieved via silane treatment. During processing, silane will hydrolyze and react with both cellulosic hydroxyl groups and matrix polymer chains, enhancing particle wettability and improving dispersion [9].

Fig. 5c shows the improvement in fiber wettability and mechanical bond achieved through MA-graft copolymerization. Through reactive extrusion, MA functional groups catalyze an esterification reaction and elicit covalent and hydrogen bond formation with the hydroxyls of cellulose [16]. The MA grafted chains will localize to the OWF and provide the OWF with a surface energy similar to the matrix phase, thus allowing good wetting of the OWF and increasing fiber dispersion within the matrix phase [13].

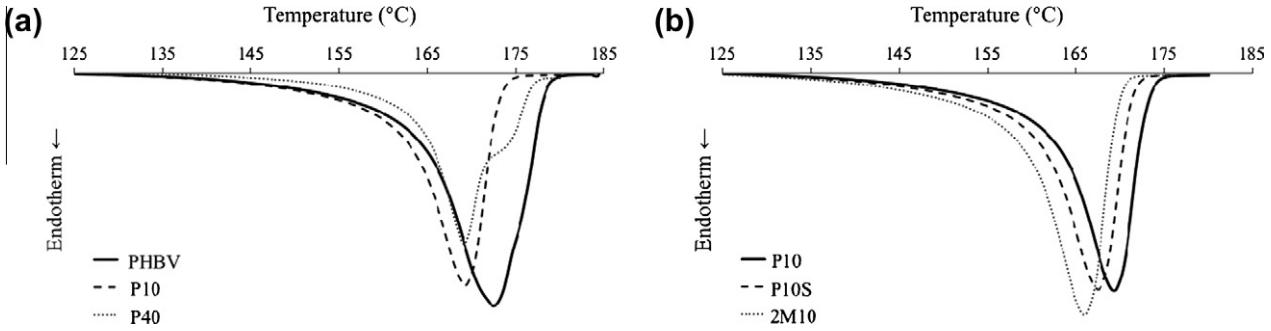

Fig. 4. DSC thermograms demonstrating the effect of (a) increasing OWF content on neat PHBV polymer and (b) compatibilizing 10 vol% PHBV/OWF composites with silane and MA on heat of melting. The scans were performed at a heating rate of 3 °C/min.

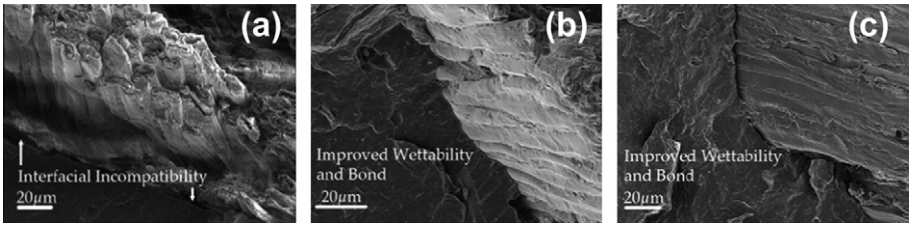

Fig. 5. SEM micrographs showing (a) the incongruous neat PHBV/untreated OWF fiber–matrix interface and improved fiber wettability achieved with compatibilization in (b) neat PHBV/silane-treated OWF and (c) mPHBV/untreated OWF.

As shown in Table 2, the reduction in matrix crystallinity is not as significant for the MA-treated PHBV as the PHBV in untreated and silane-treated composite samples. In the polymer melt, the MA-grafts, which are bulky relative to the PHBV side groups, can migrate to and orient toward the wood flour surface. The chemical bonds between fibers and MA groups reduce the transcrystalline disorder and allow the rest of the bulk PHBV matrix to crystallize without disturbance.

Inevitably, however, some MA chains would be entangled in the bulk, disrupting the crystallization of PHBV. Calorimetry results of neat PHBV and MA-grafted PHBV confirm a reduction of polymer crystallinity with the grafting of MA functional groups on the PHBV backbone. The DSC thermograms for neat PHBV and MA-grafted PHBV are shown in Fig. 6. ΔH_m decreased from 80.83 J/g for neat PHBV to 71.70 J/g for MA-grafted PHBV. This morphological change in polymer crystallinity results in a 9.6% decrease in polymer stiffness from 3800 ± 102 MPa to 3434 ± 103 MPa, an increase in elongation to break from 0.6% to 4.5%, and an increase in toughness attributed to an enhanced energy absorption capacity via HV and MA chain entanglement. The double peak of the MA-grafted PHBV melting endotherm suggests evidence of the formation of multiple morphological crystal structures and/or the phenomena of melt-recrystallization that has been shown to occur during the melting process of the neat polymers [17,30].

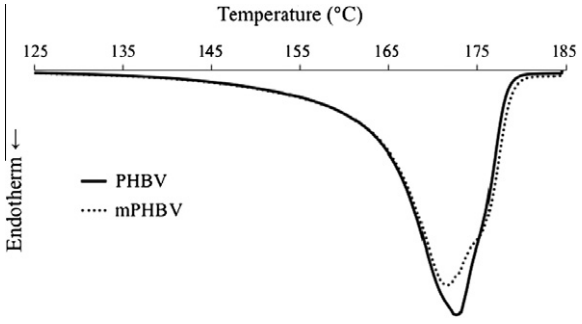

Fig. 6. Dsc thermograms for PHBV and mPHBV at a heating rate of 3 °C/min.

The initial stiffness reduction of MA-PHBV is remarkably overcome by incorporation of OWF. For example, 17 vol% OWF resulted in a composite stiffness of 4315 ± 143 MPa and 4866 ± 113 MPa for PHBV/untreated OWF and MA-grafted PHBV/untreated OWF composites, respectively, suggesting that the additional OWF surface area allows the longer MA chains to reorient and react with the hydroxyls in the cellulose, eliminating their potential to inhibit crystallization of the bulk.

Further substantiating this phenomenon, Fig. 2b shows similar heat of melting curves for silane-treated and untreated composite matrices. The 2M10 melting curve has a larger, shifted endothermic peak, suggesting MA-grafting together with the incorporation of wood flour significantly alters the crystalline matrix morphology. Since silane was thermochemically bonded only to the surface of the fiber, the process-induced fiber crushing mechanism may have negated the full potential of the silane treatment to significantly alter the matrix morphology. However, the improvements in composite stiffness and strength in both silane- and MA-compatibilized samples are ascribed to improved mechanical interlock and shear-transfer capacity obtained through better wetting of the fiber by the polymer. It is also hypothesized that improved fiber wettability and increased dispersion is responsible for the darker tints of the silane-treated and MA-grafted specimens compared to the untreated specimens, as more wood flour surface area is susceptible to charring during the injection molding process.

3.3. Micromechanical Modeling

The most widely accepted and commonly employed theoretical model for initial composite stiffness of short fiber reinforced

Table 3
Halpin-Tsai Micromechanical model parameters.

Parameters	Value	Unit	Description
l/d	3.6	–	Filler aspect ratio
E_f	6847	MPa	Filler modulus of elasticity
E_m PHBV	3800	MPa	Matrix modulus of elasticity (neat PHBV)
E_m mPHBV	3434	MPa	Matrix modulus of elasticity (M-PHBV)

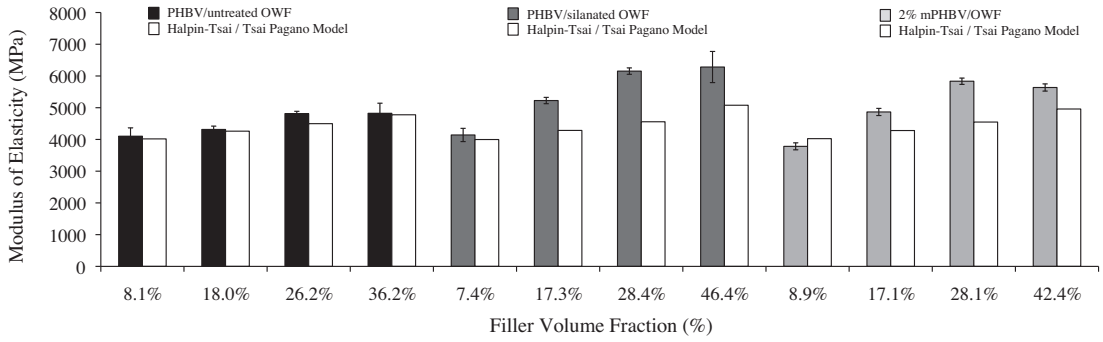

Fig. 7. Comparison of experimental results with the Halpin–Tsai/Tsai–Pagano micromechanical model for composite stiffness. The error bars show ± one standard deviation.

polymeric composites, the semi-empirical Halpin–Tsai/Tsai–Pagano equations, were used to model the global composite tensile modulus using the micromechanical properties of the individual fiber and matrix phase constituents. Using experimentally determined parameters including particle aspect ratio (l/d), filler volume fraction, and elastic matrix properties, as well as back-calculated transverse and longitudinal filler properties, this robust micromechanical modeling approach has been used previously to predict the initial stiffness of PHBV/untreated wood flour composites [31] and is similarly employed herein to validate the model for untreated specimens and to investigate its suitability for silane-treated and MA-grafted specimens. The values of transverse and longitudinal elastic properties of oak wood, however, were not experimentally derived, but rather stochastically determined by averaging published empirical mechanical values for oak wood species in the National Design Specification for Wood Construction [32]. A list of parameters and properties used in the micromechanical model calculations is presented in Table 3.

Fig. 7 shows the comparison of modulus of elasticity values determined experimentally with the initial composite stiffness predictions of the Halpin–Tsai/Tsai–Pagano model for each of the three families of composites. As can be seen in the figure, the model provides a good estimation of composite stiffness for the untreated PHBV/OWF composite specimens; however, it does not capture the enhanced stiffness improvement exhibited by the silane-treated and MA-grafted families of PHBV/OWF composites. Other studies have shown that similar implementation of the Halpin–Tsai/Tsai–Pagano model achieved good predictions for composites with low filler vol% with high l/d fillers (>100), but deviations from the model occur with low l/d fillers (<10), with high filler loading (>20%), and with silane-treated samples [33]. Similarly in this study with a low l/d filler (3.6), the model underestimates the stiffness of the resultant composites. The divergences are also more pronounced in compatibilized samples.

It is believed that the inability of the model to provide a good estimation for the silane and MA-treated composites is attributed to its failure to incorporate the effects of improved fiber wettability and dispersion and the corresponding fundamental changes in crystalline matrix morphology that occur during processing. Current research investigations include further refinement and development of new composite stiffness micromechanical models that account for treatment-induced morphological changes in the matrix microstructure.

4. Conclusions

The effects of OWF vol%, a silane coupling agent, and a MA-grafting technique on the mechanical, morphological, and thermodynamic properties of PHBV-based composites were investigated. SEM micrographs confirm a phenomenological increase in overall composite density due to the collapse or matrix infill of OWF during the injection molding process. The introduction of OWF led to an increase in composite stiffness and to decreases in strength and elongation-to-break. From the experimental results, it can be concluded that the compatibilization techniques employed caused an increase in fiber wettability and distribution, as well as enhanced mechanical interlock between fibers and the matrix phase which resulted in improved mechanical properties.

The crystallinity of neat PHBV decreased after MA-grafting via reactive extrusion, as evidenced by the marked softening of polymer stiffness, as well as the reduction in the calorimetric heat of melting, and the overall crystallinity of neat PHBV and MA-grafted PHBV decreased with the incorporation of OWF. Attributed to the migration of MA chains to the fiber–matrix interface, the crystallinity of MA-treated PHBV composite matrices decreased less than silane-treated and untreated composite matrices. Furthermore, the initial modulus softening of MA-PHBV was overcome with as little as 17 vol% OWF.

The Halpin–Tsai/Tsai–Pagano micromechanical model for initial composite stiffness showed good correlation with neat PHBV/untreated OWF composites. Disparities in the model were evident for composites with higher fiber loadings and for composites that were compatibilized with silane and MA. The differences in predicted and experimental values are attributed to the model's inability to account for increased wettability and therefore dispersion of the particulate filler and changes in the crystalline morphology of the polymer. Micromechanical models that incorporate the phenomenological alterations of the microstructure need be developed to accurately predict the global compatibilized–constituent composite behavior.

Acknowledgments

The research presented herein was sponsored by the National Science Foundation (NSF) (Grant CMMI-0900325) and supported by the NSF Graduate Research Fellowship Program, as well as the California Environmental Protection Agency's Department of Toxic Substances Control (Grant No. 07T3451). This work represents the views of the authors and not necessarily those of the sponsors. The collaboration with Aaron Michel, Anthony Alvarado, and Kristhian Morales at Stanford University is gratefully acknowledged.

References

[1] Anderson AJ, Dawes EA. Occurrence, metabolism, metabolic role, and industrial uses of bacterial polyhydroxyalkanoates. Microbiology reviews 1990; 450–72.
[2] Asenjo JA, Suk JS. Microbial (PHB): conversion of methane into poly-(hydroxybutyrate) growth and intracellular product accumulation in a Type II methanotroph. J Ferment Tech 1986;4:271–8.
[3] Morse M. Anaerobic biodegradation of biocomposites for the building industry. Doctoral Dissertation: Stanford University; 2009.

[4] Avella M. Review: properties of blends and composites based on poly(3-hydroxy)butyrate (PHB) and poly(3-hydroxybutyrate-hydroxyvalerate) (PHBV) copolymers. J Mater Sci 2000;35:523–45.
[5] Reinsch V, Kelley S. Crystallization of poly (hydroxybutyrate-co-hydroxyvalerate) in wood fiber-reinforced composites. J Appl Sci 1997;64(9):1785–96.
[6] Satyanarayana KG, Arizaga GC, Wypych F. Biodegradable composites based on lignocellulosic fibers—an overview. Prog Polym Sci 2009;34:982–1021.
[7] Dufresne A, Dupeyre D, Paillet M. Lignocellulosic flour-reinforced poly(hydroxybutyrate-covalerate) composites. J Appl Polym Sci 2003;87:1302–15.
[8] Eldsatel C, Albertsson AC, Karlsson S. Impact of degradation mechanisms on PHBV during composting. Acta Polym 1997;48:478–83.
[9] George J, Sreekala MS, Thomas S. A review on interface modification and characterization of natural fiber reinforced plastic composites. Polym Eng Sci 2001;41(9):1471–85.
[10] Wu J, Yu D, Chan C-M, Kim J, Mai Y-W. Effect of fiber pretreatment condition on the interfacial strength and mechanical properties of wood fiber/PP composites. J Appl Polym Sci 2000;76:1000–10.
[11] Javadi A, Srithep Y, Pilla S, Lee J, Gong S, Turng LS. Processing and characterization of solid and microcellular phbv/coir fiber composites. Mater Sci Eng C 2010:749–57.
[12] Shanks A, Hodzic A, Wong S. thermoplastic biopolyester natural fiber composites. J Appl Polym Sci 2004;91:2114–21.
[13] Wong S, Shanks R, Hodzik A. Interfacial improvements in PHB-flax fibre composites with hydrogen bonding additives. Comp Sci Tech 2004;64:1321–30.
[14] Shibata M, Takachiyo K-I, Ozawa K, Yosomiya R, Takeishi H. Biodegradable polyester composites reinforced with short abaca fiber. J Appl Polym Sci 2002;85:129–38.
[15] Wu C-S. Assessing biodegradability and mechanical, thermal, and morphological properties of an acrylic acid-modified poly(3-hydroxybutyric acid)/wood flours biocomposite. J Appl Polym Sci 2006;102:3565–74.
[16] Anderson S. Wood fiber reinforced bacterial biocomposites: effects of interfacial modifiers and processing on mechanical and physical properties. Doctoral Dissertation: Washington State University; 2007.
[17] Avella M, Bogoeva-Gaceva G, Buzarovska A, Errico ME, Gentile G, Grozdanov A. Poly(3-hydroxybutyrate-co-3-hydroxyvalerate)-based biocomposites reinforced with Kenaf fibers. J Appl Polym Sci 2007;104:3192–200.
[18] Jiang L, Huang J, Qian J, Chen F, Zhang J, Wolcott MP, et al. Study of Poly(3-hydroxybutyrate-co-3-hydroxyvalerate) (PHBV)/bamboo pulp fiber composites: effects of nucleation agent and compatibilizer. J Polym Environ 2008;16:83–93.
[19] Bourbon C, Karamuk E, de Fondaumiere MJ, Ruffieux K, Mayer J, Wintermantel E. Processing and characterization of a new biodegradable composite made of PHBV Matrix and regenerated cellulosic fibers. J Environ Polym Deg 1997;5(3):159–66.
[20] Chen C, Peng S, Fei B, Zhuang Y, Dong L, Feng Z, et al. Synthesis and characterization of maleated PHB. J Appl Polym Sci 2003;88:659–68.
[21] ASTM. Standard test method fortensile properties of plastics (ASTM D638). West Conshohocken, PA: American Society of Testing and Materials 2008.
[22] ASTM. Standard test methods for density and specific gravity (relative density) of plastics by displacement (ASTM D792). West Conshohocken, PA: American Society of Testing and Materials 2008.
[23] ASTM. Standard test methods forconstituent content of composite materials (ASTM D3171). West Conshohocken, PA: American Society of Testing and Materials 2009.
[24] Brandrup J, Immergut EH, Grulke EA, Abe A, Bloch DR, editors. Polymer handbook. 4th ed. John Wiley & Sons; 1999;2005.
[25] Clemons C. Wood flour. Functional fillers for plastics. Wiley-VCH Verlag GmbH & Co KGaA; 2005. p. 249–70 [chapter 5].
[26] Beckermann G. Performance of hemp-fibre reinforced polypropylene composite materials. Doctoral Dissertation: University of Waikato; 2007.
[27] Tarkow H, Southerland C. Interaction of wood with polymeric materials. US Dept of Agriculture: Forest Products Laboratory; 1964. p. 184–6.
[28] Pilla S, Gong S, O'Neill E, Rowell RM, Krzysik AM. Polylactide-pine wood flour composites. Polym Eng Sci 2008:578–87.
[29] Abdemouleh M, Boufi S, Belgacem MN, Dufresne A. Short natural-fibre reinforced polyethylene and natural rubber composites: effect of silane coupling agents and fibres loading. Comp Sci Technol 2007;67:1627–39.
[30] Wei CL, Chen M, Yu FE. Temperature modulated DSC and DSC studies on the origin of double melting peaks in poly(ether ether ketone). Polymer 2003;44:8185–93.
[31] Singh S, Mohanty AK. Wood fiber reinforced bacterial bioplastic composites-fabrication and performance evaluation. J Comp Sci Technol 2007;67:1753–63.
[32] American Forest and Paper Association. National design specification (NDS) for wood construction. Washington, DC, 2005.
[33] Pilla S, Gong S, O'Neill E, Yang L, Rowell RM. Polylactide-recycled wood fiber composites. J Appl Polym Sci 2008;111:37–47.